The temperature-dependency of the optical band gap of ZnO measured by electron energy-loss spectroscopy in a scanning transmission electron microscope

Cecilie S. Granerød, Augustinas Galeckas, Klaus Magnus Johansen, Lasse Vines, and Øystein Prytz
Department of Physics, Centre for Materials Science and Nanotechnology, University of Oslo, P.O. Box 1048, Blindern, N-0316 Oslo, Norway

(Received 23 January 2018; accepted 29 March 2018; published online 13 April 2018)

The optical band gap of ZnO has been measured as a function of temperature using Electron Energy-Loss Spectroscopy (EELS) in a (Scanning) Transmission Electron Microscope ((S)TEM) from approximately 100 K up towards 1000 K. The band gap narrowing shows a close to linear dependency for temperatures above 250 K and is accurately described by Varshni, Bose-Einstein, Pässler and Manoogian-Woolley models. Additionally, the measured band gap is compared with both optical absorption measurements and photoluminescence data. STEM-EELS is here shown to be a viable technique to measure optical band gaps at elevated temperatures, with an available temperature range up to 1500 K and the benefit of superior spatial resolution. *Published by AIP Publishing.*
https://doi.org/10.1063/1.5023316

I. INTRODUCTION

The band gap is a fundamental property of semiconductors, and control and manipulation of the optical band gap is of increasing interest both from a scientific view and for development of new applications.[1–3] This has led to the field of band gap engineering, where the optical band gap is manipulated through alloying or nanoscale modification of the structure.

Optical band gaps are typically monitored by either absorption or luminescence of light in the infrared to ultraviolet spectral range.[4] The achievable lateral resolution of these types of techniques is, however, limited by the wavelength of the light. Hence, the growing interest in band gap engineering on the nanometer scale is therefore posing certain challenges to these optical characterization methods, where the signal is effectively spatially averaged. A recent trend is to use Scanning Transmission Electron Microscopy (STEM) in combination with Electron Energy-Loss Spectroscopy (EELS). If the EELS experiment is set up to allow only small momentum transfer, the measured energy loss spectra in EELS correspond closely to the optical absorption coefficient as measured in optical absorption spectroscopy, and the optical band gap can similarly be found from the onset of energy loss.[5] Previously, these energy loss onsets have been mapped with excellent spatial resolution using STEM-EELS, thereby allowing direct access to the optical band gap at the length scales relevant to modern semiconductor device nanostructuring and band gap engineering.[1,6–8]

The band gap energy is predetermined by the structure and the chemical composition of the material and can be affected by factors such as pressure (strain/stress) and temperature. Increasing the temperature typically leads to a decrease in the band gap energy, caused by a combination of thermal lattice expansion[9,10] and the temperature-dependency of the electron-phonon interaction.[11–13] This effect becomes particularly important when the device in question is intended to operate at elevated temperatures.[14] Knowledge of temperature dependence of the band gap is also essential for controlling the desired electrical and optical properties through thermal processing, e.g., the point defect formation energy depends on the change in the band gap, which indirectly influences the resulting electrical properties and dopant diffusion behavior of the material.[2,15–17]

It is challenging to measure the optical band gap values at elevated temperatures with conventional methods, especially with emission-based techniques such as photoluminescence (PL) and cathodoluminescence (CL).[18–20] CL may in some cases also probe band gap variation with spatial resolution on the nanoscale; however, the non-radiative recombination of electron-hole pairs, and/or thermal quenching of radiative channels, effectively limit the emission of light, and thereby also the suitability of these techniques at elevated temperatures. In order to obtain the band gap values at elevated temperatures, one option is then to extrapolate the low temperature data to high temperatures by the use of various empirical models for the temperature dependency. These models include the Varshni, Pässler, Bose-Einstein, or Manoogian-Wooley models.[21–29] However, high-temperature extrapolation based on these models is highly questionable, as small differences in low-temperature data result in wildly differing extrapolated values, and an unacceptably large scatter in predicted band gap energies.[18,20,30–36] Absorption based techniques are, on the other hand, not limited by temperature; however, very few studies exists for temperatures above 800 K.[19] As these temperatures are relevant to thermal processing,[37] accurate knowledge of the optical band gap may be crucial, which illustrates the importance of direct measurements at relevant temperatures.

In this work, we demonstrate the capability of EELS to determine the temperature-dependent optical band gap of wide band gap materials over a large temperature range, which can be combined with high resolution recordings. This is

exemplified by zinc oxide (ZnO), which is a technologically important wide band gap oxide with promising properties for optoelectronic applications—potentially working at elevated temperatures. The material is known to have a strong dependence of the band gap as a function of temperature,[38] and therefore provide a good test case for developing the technique. ZnO is also technologically important in its own right and as a platform for a variety of alloys, such as MgZnO[39] and CdZnO,[40] and thus accurate knowledge and control of optical parameters is imperative. Here, we determine the temperature dependence of the optical band gap up towards 1000 K, and the corresponding fitting parameters for the most widely used band gap models are precisely extracted. The results are compared with optical absorption measurements and literature data, demonstrating that the current approach can achieve both high precision and good accuracy, thereby pointing towards future applications where the optical band gap of nanostructured devices can be investigated at both relevant length scales and temperatures.

II. EXPERIMENTAL

The *in-situ* cooling experiments were performed with a Gatan 636 Liquid Nitrogen cryoholder. The dewar was evacuated and baked out for several hours to provide maximum cooling and temperature stability. The *in-situ* heating experiments were performed with an FEI NanoEX single tilt MEMS based heating holder,[41] with a temperature readout accuracy listed at 4%, and a temperature precision on the order of 0.1 K. In both cases, TEM specimens were prepared by crushing a high quality single crystal of ZnO from Tokyo Denpa in ethanol in a mortar before being deposited on standard holey carbon copper grids and the dedicated heating chips of the NanoEX holder. During the experiments, particles of different sizes, thicknesses, and at different locations were used in STEM-EELS measurements to avoid potential artefacts.

The EELS experiments were performed using an FEI Titan G2 60–300 kV transmission electron microscope equipped with a monochromator and a probe corrector. With the monochromator strongly excited, high energy resolution is obtained at the expense of beam intensity. The microscope was operated at the lowest acceleration voltage of 60 kV in order to increase the interaction cross-section, thus increasing the EELS edge intensity relative to the background, in addition to reducing the generation of Cherenkov radiation.[42] The STEM convergence angle was set to 30 mrad, and the electron energy loss was measured with a Gatan Quantum 965 GIF with a collection angle of 27 mrad. With a dispersion of 0.01 eV/channel, the system energy resolution was found to be approximately 110 meV, as measured by the full-width-half-maximum (FWHM) of the zero-loss peak (ZLP); the direct signal originating from electrons passes through the sample without any significant energy loss. The exposure time was set to around 0.001 s, as a compromise between increasing the signal-to-noise ratio and avoiding reduced energy resolution due to fluctuations caused by external electromagnetic fields.

The temperature dependency was obtained by measuring STEM-EELS at predefined temperature steps, with a large time span between each step in order to stabilize the temperature and the sample drift. The STEM-EELS acquisition was set up to collect spectral images, where full spectra were collected at each pixel within a two-dimensional raster scan across the sample. Directly after each acquisition, the spectral images were corrected by normalizing with the dark current in order to suppress variances in detector gain. Each individual spectrum in the 2D scan was calibrated by aligning the zero-loss peak at 0 eV, and the spectral images were summed to produce a single spectrum for each temperature step. The background, consisting of a large tail from the ZLP, was subtracted in each temperature step by fitting a model for the background to the intensity immediately in front of the edge, and extrapolating it beyond the edge onset. A fitting range of 0.3 eV was used, and both the standard decaying power-law model and a linear model were tested. The two models gave no significant difference in the extracted band gap, and in the end, the linear model was used for the whole data set.

Temperature-dependent measurements of photoluminescence (PL) and band-edge absorption were carried out in the range 10 K–325 K by employing a closed-cycle He refrigerator system and using a 325 nm wavelength cw He-Cd laser as an excitation source. The transmittance spectra were recorded with a fiber optic spectrometer (Ocean Optics HR4000, spectral resolution 0.2 nm), transformed into absorption spectra, and the optical band gaps were found by extracting the edge onsets using Tauc plots.[43] In optical emission and absorption experiments, ZnO material in the form of a thin film grown by Molecular Beam Epitaxy (MBE) and a bulk crystal (commercial hydrothermally (HT) grown ZnO wafer) has been examined.

III. RESULTS AND DISCUSSION

In order to determine a suitable temperature range for the band gap measurements, a ZnO particle was monitored by STEM as a function of increasing temperature. The STEM observation indicated that morphological changes start to occur at temperatures above 1100 K, and at 1300 K, the particle appears entirely decomposed, as shown in Fig. 1. Hence, to avoid sample degradation during the heating experiments, the upper limit for the temperature was set to about 975 K.

Furthermore, the effect of local beam heating was investigated using the script by Mitchell and Bertram, based on the beam heating equation developed by Egerton.[44] With relevant parameters and ZnO properties,[45,46] the local heating of the converged STEM beam was estimated to be less than 0.1 K, and thus is negligible.

Typical results of the temperature-dependent EELS measurements after background subtraction are shown in Fig. 2. A full-scale raw EEL spectrum is illustrated in the inset, where a characteristic step-like feature (marked by a shaded rectangular region) is related to electron transitions from the valence to conduction band. Considering the room temperature (RT, 300 K) spectra in Fig. 2 as reference, one can observe that cooling down to 100 K blue-shifts the energy-loss edge towards higher energies, which is consistent with band gap broadening, and also steepens the edge. Conversely, when heating the sample to 875 K, the onset red-shifts, i.e., lead to band gap

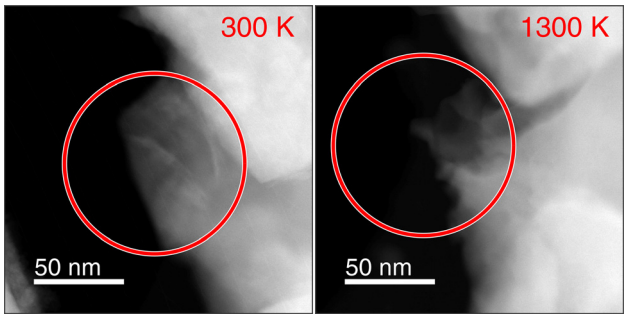

FIG. 1. STEM annular dark field images of a representative ZnO particle (marked by the red circle) at 300 K and at 1300 K, where it gets decomposed.

narrowing, while also showing a less steep edge. To ensure that high-temperature treatment of the sample in vacuum did not affect the ZnO material properties irreversibly, EELS was measured at RT both before and after heating to 975 K. This is indeed confirmed in Fig. 2, where the heat treatment left the edge unaffected in both shape and position.

For materials with a direct band gap, the onset of the electron energy-loss is related to the optical band gap. This is similar to the onset of absorption in optical absorption experiments, which are commonly analyzed by Tauc plots. Correspondingly, the assessment of the optical band gap in EELS relies on curve fitting the energy-loss edge within a suitable range to identify the onset. In the following, we will assume that the band structure of ZnO can be described by a parabolic valence band and a conduction band separated by a direct gap E_g. Then, considering all direct transitions, the equivalent to a Tauc method in EELS is given by[5]

$$[I(E)]^2 = c(E - E_g), \tag{1}$$

where $I(E)$ is the measured signal intensity as a function of energy loss E. One important distinction between optical experiments and EELS is that transitions with significant momentum transfer can occur in EELS. In principle, this can cause the shape of the energy loss intensity to deviate from the model in Eq. (1). However, we have previously[8] found that this model gives a high goodness of fit ($R^2 > 0.97$) for ZnO, and furthermore that the extracted band gap is close to that found by optical methods.[1] With c and E_g as fitting parameters, the curve fit of Eq. (1) to the spectra in Fig. 2 results in extracted onset values of 3.33 eV at 100 K, 3.28 eV at RT, and 3.06 eV at 875 K ($R^2 > 0.98$ for all analyzed spectra).

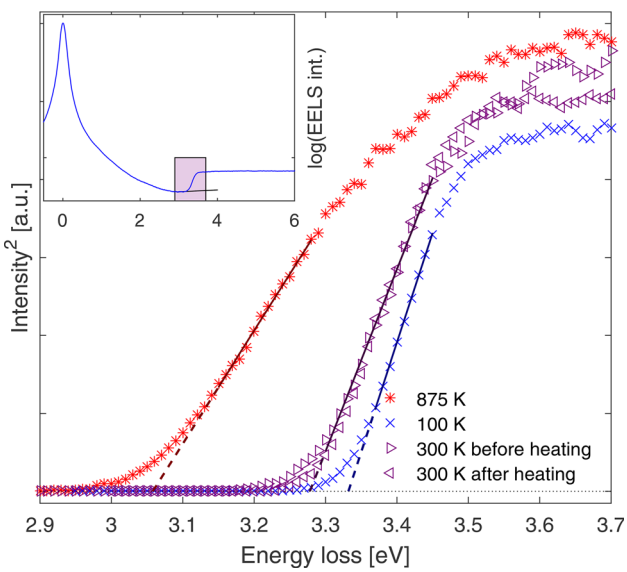

FIG. 2. Background-subtracted EEL spectra at different temperatures, and before/after the heating experiment (squared intensity). The inset shows the raw EEL spectrum at 100 K (log scale) with background fitting.

A series of 7 measurements were performed at RT on different particles and under slightly different experimental conditions to statistically validate the results, yielding the average onset of 3.27 eV with a standard deviation of 0.01 eV. This agrees well with the commonly reported ZnO optical band gap value at RT by UV-visible absorption methods.[47] The measurements were performed on particles with different sizes in the range from approximately 50 nm towards 200 nm (measured on a thin part of the particle). With small particles, quantum confinement may influence the band gap; however, this effect has previously been observed in particles below 15 nm.[48,49] As the particles in this work are 50 nm and larger, no size dependency with onset was observed, as expected. Additionally, the standard deviation found here is similar to the accuracy of the energy calibration, which is 0.01 eV by the experimental dispersion. Hence, this is a reasonable estimation for the uncertainty in the band gaps.

Figure 3 shows the temperature-dependency of the ZnO onset measured by EELS in the range 100–975 K. The error bars represent the standard deviation, as found above. Similar temperature-dependencies of the ZnO optical band gap reported in the literature using the two most common methods are also included; references using PL (which refers to the A exciton peak position)[18,30–36] and optical absorption spectroscopy[20] are also presented in the plot, along with the corresponding extrapolation to higher temperatures. A small difference in offset between the experiment and some of the results in the literature can be observed and is discussed below, whereas the relative shift is measured accurately compared to the extrapolations of the literature data. As expected, the values from previous studies recorded at low temperatures and extrapolated towards higher temperatures scatter over a large range, e.g., in a range from 2.75 up to 3.15 eV at 1000 K. In other words, measurement at the relevant temperature is necessary. In contrast, the STEM-EELS provides experimental data for the ZnO onset up towards 1000 K, with a value of 3.01 eV at 1000 K.

One of the very few measurements of the ZnO optical band gap performed at elevated temperatures was done by Hauschild *et al.*[19] Only the relative shift in the optical band gap is presented, where a relative shift of approximately −0.33 eV in the range 100–800 K is observed. This is comparable to the EELS results, where we find a relative shift of −0.24 eV in the same temperature range.

From the results shown in Fig. 3, the necessity of highly accurate modeling parameters is obvious. The band gap variation with temperature is usually attributed to thermal lattice expansion and temperature-dependent phonon-electron interaction, and here, common temperature-dependent band gap

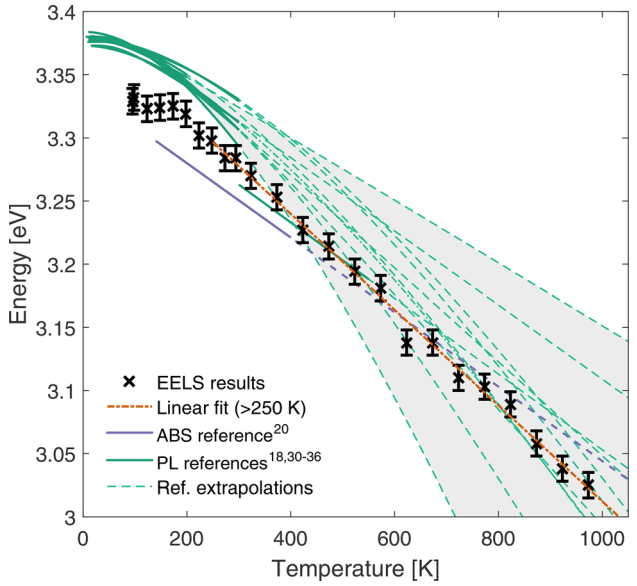

FIG. 3. Temperature dependent band gap of ZnO assessed by different techniques. EELS edge onset energy as a function of temperature, with the linear fit above 250 K. References from optical absorption (ABS) onset energy[20] and photoluminescence (PL) exciton A emission energy[18,30–36] within the corresponding measured temperature range (lines), and extrapolation from the curve fits (dashed).

models are reviewed in detail. At elevated temperatures, the band gap E_g shifts linearly with temperature T, and can accordingly be fitted as

$$E_g(T) = E_g(0) - \alpha T. \tag{2}$$

At lower temperatures, a quadratic dependency with temperature is expected,[11] and this is indeed observed on the low-temperature side of the EELS results. For the linear function in Eq. (2), one can choose to avoid this region and perform the fitting only at higher temperatures, as shown in Fig. 3. Alternatively, the empirical Varshni expression[21] is by far the most commonly used to fit the temperature-dependent band gap, by

$$E_g(T) = E_g(0) - \alpha \frac{T^2}{T+\beta}, \tag{3}$$

where α and β are fitting parameters. Yet, another frequently used approach is to employ the Bose-Einstein relation[22–24]

$$E_g(T) = E_g(0) - \alpha \frac{\Theta_E}{e^{\Theta_E/T} - 1}, \tag{4}$$

which is based on the phonon-electron interaction. Here, the Einstein temperature Θ_E is related to the Debye temperature by $\Theta_D = \frac{4}{3}\Theta_E$. Using the temperature dependence of the optical band gap found by EELS as input, the resulting fit parameters of these models are listed in Table I. Here, the linear fit above 250 K results in the gradient of 0.38 meV/K, which is assumed to be a good estimate for further interpolation and extrapolation of high-temperature band gaps of ZnO. However, with the full range of the data set, the Bose-Einstein fit reaches a higher goodness-of-fit (R^2) and may therefore be the preferred model. Furthermore, the fitted Einstein temperature of Eq. (4) suggests a Debye temperature of 519 K. As the Debye temperature for ZnO is reported in the range from 416 K[50] up to 920 K,[51] this shows good agreement between our results and theoretical estimates for Θ_D.

Less commonly used, but more advanced models, can also be applied to the temperature-dependent ZnO band gap. The model proposed by Pässler introduces an additional fitting parameter, and is given by[25,26]

$$E_g(T) = E_g(0) - \frac{\alpha\Theta_P}{2}\left[\sqrt{1 + \left(\frac{2T}{\Theta_P}\right)^q q} - 1\right], \tag{5}$$

where p and Θ_P are empirical parameters. Alternatively, as proposed by Manoogian and Woolley, the Bose-Einstein model can be improved by including a term for the thermal lattice expansion, which can be expressed by[27–29]

$$E_g(T) = E_g(0) - UT^s - V\frac{\Theta_E}{e^{\Theta_E/T} - 1} \tag{6}$$

with s as the exponent of the thermal lattice expansion with coefficient U. The fitted parameters of these models are also listed in Table I. As seen by the range of 95% confidence intervals, the error is higher as compared to the simpler models described above. Hence, these models may be less suitable to describe the EELS measurements, which may be assigned to the lack of data below 100 K. However, from the fit of Eq. (6), the Debye temperature becomes $\Theta_D = 617$ K, which again compares well with the range of theoretical estimates.[50,51]

Figure 4 shows the temperature-dependent band gap values from EELS measurements up to 300 K, along with the fitting curves using the models described above. With the obvious exception of the linear fit, all models capture the weaker dependency on the temperature of the band gap observed when the

TABLE I. EELS fitting parameters for the temperature dependency of the ZnO band gap. The values in parentheses are 95% confidence intervals of the fitting.

Fit type	E_g (0) (eV)	Gradient (meV/K)	Other fit parameters	R^2
Equation (2) (Linear)	3.38 (3.37, 3.39)	$\alpha = 0.36$ (0.35, 0.38)	…	0.995
Equation (2) T > 250 K	3.39 (3.38, 3.40)	$\alpha = 0.38$ (0.37, 0.39)	…	0.995
Equation (3) (Varshni)	3.35 (3.34, 3.36)	$\alpha = 0.41$ (0.37, 0.45)	$\beta = 215$ (80, 350) K	0.996
Equation (4) (B.-E.)	3.34 (3.33, 3.34)	$\alpha = 0.40$ (0.38, 0.42)	$\Theta_E = 389$ (273, 506) K	0.997
Equation (5) (Pässler)	3.33 (3.32, 3.33)	$\alpha = 0.38$ (0.37, 0.39)	$q = 39$ (−462, 540)	0.997
			$\Theta_P = 338$ (296, 380) K	
Equation (6) (M.-W.)	3.35 (0.05, 6.64)	$U = 0.82$ (−881, 883)	$s = 0.58$ (−173, 174)	0.997
		$V = 0.37$ (−11.2, 11.9)	$\Theta_E = 463$ (−1518, 2444) K	

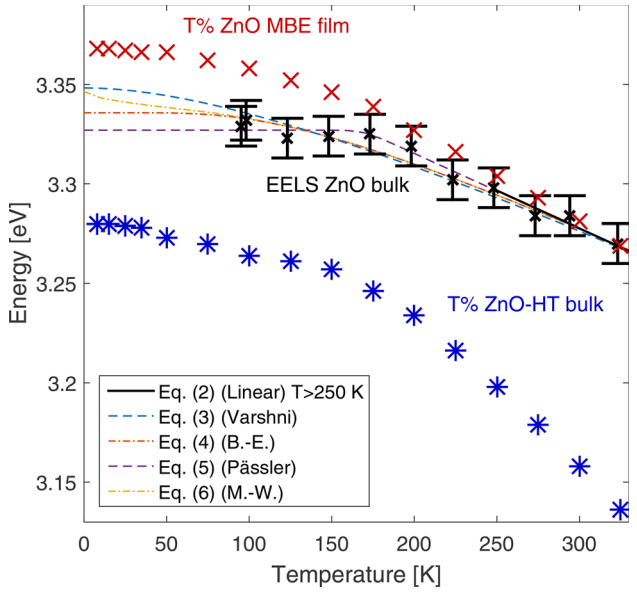

FIG. 4. ZnO EELS edge onset energy as a function of temperature, fitted with linear, Varshni, Bose-Einstein, Manoogian-Wooley, and Pässler models. Equations and fit parameters are given in the text. Corresponding measurements from optical transmission spectroscopy on an MBE-grown film and a bulk ZnO sample are included for comparison, with the energy of onset of optical absorption with temperature.

temperature is reduced below 200 K. In addition to the EELS measurements, the results of optical transmission spectroscopy have also been included. The optical transmission spectroscopy measurements were carried out on a thin film sample grown by MBE and on a bulk ZnO sample. The results in Fig. 4 show that the EELS results agree well with the transmission spectroscopy results.

Interestingly, there is a variation in the optical band gaps, both between the EELS results and the literature as shown in Fig. 3, but also from transmission spectroscopy measured on different samples shown in Fig. 4. The observed variation may be linked to several effects, or a combination thereof; e.g., the strong excitonic features of ZnO are known to interfere with the assessment of the band gap, and depending on the broadness of the exciton, this typically leads to a lower onset in absorption measurements than PL. Differences may also originate from the ZnO material, either due to impurities and defects, or potentially due to geometrical differences between the studied samples. Furthermore, differences originating from the characterization technique and/or the probing depth, where emission, absorption, spectroscopic ellipsometry, etc., all may interact differently with the material, may also lead to a certain variation. Finally, the band gap extraction method could also lead to differences, especially related to Tauc plots.[47] Thus, the variation in the reported band gaps is a topic of studies on its own.[4,47,52] However, as can be seen from Figs. 3 and 4, the measured data in this study fall well within the range of experimentally reported band gaps in the literature.

In summary, the EELS results of ZnO show a clear shift in the optical band gap with temperature, which is also evident from the raw data. This shift is found to be reversible with temperature within the studied temperature range, from approximately 100 K to 1000 K. This further supports that the observed change originates from changes in the band gap. Prospective models have been fitted to the measured band gap as a function of temperature and result in good fits between the models and the experimental data. As the band gaps are also well within the range of band gaps found by other techniques in the literature, we conclude that EELS can successfully be used to determine band gaps as a function of temperature. Finally, it can be noted that the full potential of STEM-EELS can be attained by exploiting the nanoscale spatial resolution of band gap measurements, which opens up avenues for the measurement of small features and nanostructures which cannot be obtained with the comparable optical techniques.

IV. CONCLUSIONS

STEM-EELS has been proven to be a successful technique for the determination of optical band gaps and its variation with temperature in a wide range. This has been validated by measurements on ZnO from 100 K to 1000 K, and several well-established models were applied for fitting the measured temperature dependencies, yielding relevant parameters for accurate prediction of the ZnO band gap development. Here, we find that for temperatures above 250 K, the band gap can be linearly fitted by a gradient of 0.38 meV/K. While this work demonstrates the correspondence between EELS and more conventional methods based on optical absorption and emission, the nanoscale spatial resolution of STEM-EELS provides a unique opportunity for measuring nanostructures that is not available with any other technique.

ACKNOWLEDGMENTS

This work was supported by the Faculty of Mathematics and Natural Sciences via the strategic research program Foxhound. The Research Council of Norway is acknowledged for the support offered to the frontier research project FUNDAMeNT (Grant No. 251131), the Norwegian Center for Transmission Electron Microscopy (NORTEM) (Grant No. 197405/F50), and the Norwegian Micro- and Nano-Fabrication Facility (NorFab) (Grant No. 245963/F50). In addition, Sindre R. Bilden is acknowledged for useful discussions.

[1]W. Zhan, C. S. Granerød, V. Venkatachalapathy, K. M. Johansen, I. J. T. Jensen, A. Y. Kuznetsov, and Ø. Prytz, Nanotechnology **28**, 105703 (2017).
[2]A. Janotti and C. G. V. d. Walle, Rep. Prog. Phys. **72**, 126501 (2009).
[3]Q. Fang Li and J.-L. Kuo, J. Appl. Phys. **114**, 063715 (2013).
[4]V. Srikant and D. R. Clarke, J. Appl. Phys. **83**, 5447 (1998).
[5]B. Rafferty and L. M. Brown, Phys. Rev. B **58**, 10326 (1998).
[6]M. Bosman, L. J. Tang, J. D. Ye, S. T. Tan, Y. Zhang, and V. J. Keast, Appl. Phys. Lett. **95**, 101110 (2009).
[7]L. Gu, W. Sigle, C. T. Koch, J. Nelayah, V. Srot, and P. A. van Aken, Ultramicroscopy **109**, 1164 (2009).
[8]C. S. Granerød, W. Zhan, and Ø. Prytz, Ultramicroscopy **184**, 39 (2018).
[9]W. Shockley and J. Bardeen, Phys. Rev. **77**, 407 (1950).
[10]J. Bardeen and W. Shockley, Phys. Rev. **80**, 72 (1950).
[11]T. Muto and S. Ôyama, Prog. Theor. Phys. **5**, 833 (1950).
[12]H. Y. Fan, Phys. Rev. **78**, 808 (1950).
[13]H. Y. Fan, Phys. Rev. **82**, 900 (1951).
[14]P. G. Neudeck, R. S. Okojie, and L.-Y. Chen, Proc. IEEE **90**, 1065 (2002).
[15]T. N. Sky, K. M. Johansen, H. N. Riise, B. G. Svensson, and L. Vines, J. Appl. Phys. **123**, 055701 (2018).
[16]T. S. Bjørheim, S. Erdal, K. M. Johansen, K. E. Knutsen, and T. Norby, J. Phys. Chem. C **116**, 23764 (2012).

[17]Y. K. Frodason, K. M. Johansen, T. S. Bjørheim, B. G. Svensson, and A. Alkauskas, Phys. Rev. B **95**, 094105 (2017).
[18]D. M. Bagnall, Y. F. Chen, Z. Zhu, T. Yao, M. Y. Shen, and T. Goto, Appl. Phys. Lett. **73**, 1038 (1998).
[19]R. Hauschild, H. Priller, M. Decker, J. Brückner, H. Kalt, and C. Klingshirn, Phys. Status Solidi C **3**, 976 (2006).
[20]M. Caglar, Y. Caglar, S. Aksoy, and S. Ilican, Appl. Surf. Sci. **256**, 4966 (2010).
[21]Y. P. Varshni, Physica **34**, 149 (1967).
[22]P. Lautenschlager, M. Garriga, S. Logothetidis, and M. Cardona, Phys. Rev. B **35**, 9174 (1987).
[23]L. Viña, S. Logothetidis, and M. Cardona, Phys. Rev. B **30**, 1979 (1984).
[24]K. P. O'Donnell and X. Chen, Appl. Phys. Lett. **58**, 2924 (1991).
[25]R. Pässler, Phys. Status Solidi B **200**, 155 (1997).
[26]R. Pässler, Phys. Rev. B **66**, 085201 (2002).
[27]A. Manoogian and J. C. Woolley, Can. J. Phys. **62**, 285 (1984).
[28]A. Manoogian and A. Leclerc, Can. J. Phys. **57**, 1766 (1979).
[29]G. Fonthal, L. Tirado-Mejia, J. I. Marin-Hurtado, H. Ariza-Calderon, and J. G. Mendoza-Alvarez, J. Phys. Chem. Solids **61**, 579 (2000).
[30]C. Boemare, T. Monteiro, M. J. Soares, J. G. Guilherme, and E. Alves, Phys. B: Condens. Matter **308–310**, 985 (2001).
[31]H. J. Ko, Y. F. Chen, Z. Zhu, T. Yao, I. Kobayashi, and H. Uchiki, Appl. Phys. Lett. **76**, 1905 (2000).
[32]L. Wang and N. C. Giles, J. Appl. Phys. **94**, 973 (2003).
[33]S. Ozaki, T. Mishima, and S. Adachi, Jpn. J. Appl. Phys., Part 1 **42**, 5465 (2003).
[34]B. Cao, W. Cai, and H. Zeng, Appl. Phys. Lett. **88**, 161101 (2006).
[35]N. Kumar, R. Kaur, and R. M. Mehra, J. Lumin. **126**, 784 (2007).
[36]S. F. Chichibu, A. Tsukazaki, M. Kawasaki, K. Tamura, Y. Segawa, T. Sota, and H. Koinuma, Appl. Phys. Lett. **80**, 2860 (2002).
[37]K. M. Johansen, L. Vines, T. S. Bjørheim, R. Schifano, and B. G. Svensson, Phys. Rev. Appl. **3**, 024003 (2015).
[38]C. Jagadish and S. J. Pearton, *Zinc Oxide Bulk, Thin Films and Nanostructures: Processing, Properties, and Applications* (Elsevier, 2011).
[39]A. Ohtomo, M. Kawasaki, I. Ohkubo, H. Koinuma, T. Yasuda, and Y. Segawa, Appl. Phys. Lett. **75**, 980 (1999).
[40]L. Li, Z. Yang, Z. Zuo, J. H. Lim, and J. L. Liu, Appl. Surf. Sci. **256**, 4734 (2010).
[41]L. Mele, S. Konings, P. Dona, F. Evertz, C. Mitterbauer, P. Faber, R. Schampers, and J. R. Jinschek, Microsc. Res. Tech. **79**, 239 (2016).
[42]M. Stöger-Pollach and P. Schattschneider, Ultramicroscopy **107**, 1178 (2007).
[43]J. Tauc, R. Grigorovici, and A. Vancu, Phys. Status Solidi B **15**, 627 (1966).
[44]R. F. Egerton, P. Li, and M. Malac, Micron **35**, 399 (2004).
[45]R. A. Voronkov, R. A. Rymzhanov, N. A. Medvedev, and A. E. Volkov, Nucl. Instrum. Methods Phys. Res., Sect. B **365**, 468 (2015).
[46]X. Wu, J. Lee, V. Varshney, J. L. Wohlwend, A. K. Roy, and T. Luo, Sci. Rep. **6**, 22504 (2016).
[47]B. D. Viezbicke, S. Patel, B. E. Davis, and D. P. Birnie, Phys. Status Solidi B **252**, 1700 (2015).
[48]J. C. Nie, J. Y. Yang, Y. Piao, H. Li, Y. Sun, Q. M. Xue, C. M. Xiong, R. F. Dou, and Q. Y. Tu, Appl. Phys. Lett. **93**, 173104 (2008).
[49]K.-F. Lin, H.-M. Cheng, H.-C. Hsu, L.-J. Lin, and W.-F. Hsieh, Chem. Phys. Lett. **409**, 208 (2005).
[50]R. A. Robie and J. L. Edwards, J. Appl. Phys. **37**, 2659 (1966).
[51]A. R. Hutson, J. Phys. Chem. Solids **8**, 467 (1959).
[52]F. Li, C. Liu, Z. Ma, and L. Zhao, Opt. Mater. **34**, 1062 (2012).